

Precisely tunable magnetic phase transition temperature, T_C , through formation of molecule alloy in $[\text{Ni}_x\text{Pt}_{1-x}(\text{mnt})_2]^-$ -based spin systems ($\text{mnt}^{2-} = \text{maleonitriledithiolate}$, $x = 0.09\text{-}0.91$)

Guo-Jun Yuan,^a Hao Yang,^a Shao-Xian Liu,^a Jian-Lan Liu^a and Xiao-Ming Ren^{*a,b}

^a State Key Laboratory of Materials-Oriented Chemical Engineering and College of Science, Nanjing University of Technology, Nanjing 210009

^b College of Materials Science and Engineering, Nanjing University of Technology, Nanjing 210009

Tel.: +86 25 58139476

Fax: +86 25 58139481

Email: xmren@njut.edu.cn(RXM)

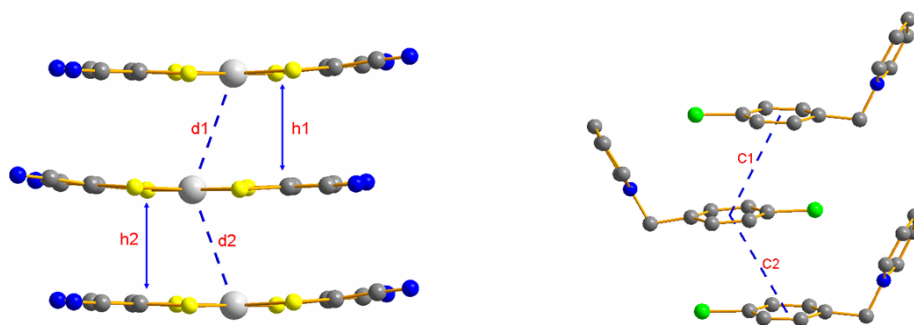
ahchljygj@163.com (YGJ)

yh2412@126.com (YH)

sxliu@njut.edu.cn (LSX)

njutljl@163.com (LJL)

Table S1 Inter-plane distances between the nearest neighbors (h1, h2) and interatomic distances of M...M (d1, d2), S...S (m1, m2, m3, m4) and the centroid-to-centroid distances (c1, c2), within an anionic or cation stack for alloy compounds [Cl-BzPy][Ni_xPt_{1-x}(mnt)₂] (x = 0.9-0.91) with the parent compounds at 296 K.



| Molar fraction | h1 | h2 | d1 | d2 | c1 | c2 |
|--------------------|-------|-------|-------|-------|--------|-------|
| x = 0 ² | 3.633 | 3.602 | 3.885 | 3.885 | 4.168 | 4.168 |
| x = 0.09 | 3.643 | 3.634 | 3.920 | 3.930 | 4.201) | 4.201 |
| x = 0.21 | 3.580 | 3.616 | 3.884 | 3.884 | 4.152 | 4.152 |
| x = 0.34 | 3.616 | 3.593 | 3.897 | 3.897 | 4.161 | 4.160 |
| x = 0.42 | 3.603 | 3.574 | 3.892 | 3.892 | 4.142 | 4.142 |
| x = 0.54 | 3.572 | 3.607 | 3.901 | 3.901 | 4.145 | 4.145 |
| x = 0.64 | 3.611 | 3.577 | 3.916 | 3.916 | 4.155 | 4.155 |
| x = 0.73 | 3.558 | 3.591 | 3.904 | 3.904 | 4.141 | 4.141 |
| 0.84 | 3.553 | 3.585 | 3.912 | 3.912 | 4.139 | 4.139 |
| x = 0.91 | 3.548 | 3.582 | 3.913 | 3.913 | 4.138 | 4.138 |
| x = 1 ⁴ | 3.575 | 3.539 | 3.914 | 3.914 | 4.133 | 4.133 |

| Molar fraction | m1 | m2 | m3 | m4 | m |
|--------------------|-------|-------|-------|-------|-------|
| x = 0 ³ | 3.986 | 4.079 | 3.883 | 3.705 | 3.913 |
| x = 0.09 | 3.941 | 3.713 | 4.068 | 4.100 | 3.956 |
| x = 0.21 | 4.080 | 3.996 | 3.698 | 3.892 | 3.916 |
| x = 0.34 | 3.905 | 3.703 | 4.019 | 4.077 | 3.926 |
| x = 0.42 | 3.904 | 3.704 | 4.020 | 4.063 | 3.922 |
| x = 0.54 | 4.076 | 4.029 | 3.712 | 3.912 | 3.932 |

| | | | | | |
|--------------------|-------|-------|-------|-------|-------|
| x = 0.64 | 3.927 | 3.726 | 4.050 | 4.084 | 3.947 |
| x = 0.73 | 4.064 | 4.046 | 3.714 | 3.914 | 3.935 |
| x = 0.84 | 4.063 | 4.058 | 3.728 | 3.916 | 3.941 |
| x = 0.91 | 4.058 | 4.065 | 3.729 | 3.915 | 3.942 |
| x = 1 ¹ | 4.050 | 4.069 | 3.734 | 3.910 | 3.941 |

References

1. X. M. Ren, Q. J. Meng, Y. Song, C. S. Lu, C. J. Hu, X. Y. Chen, *Inorg. Chem.* 2002, **41**, 5686.
2. X. M. Ren, H. Okudera, R. K. Kremer, Y. Song, C. He, Q. J. Meng, P. H. Wu, *Inorg. Chem.* 2004, **43**, 2569.

Figure S1 Variations of interatomic or interplane distances between neighboring anions in a stack (c1, c2, d1, d2, h1 and h2) as x change for [Cl-BzPy][Ni_xPt_{1-x}(mnt)₂] (x = 0.09-0.91) with two parent compounds at ambient temperature.

Table S2 Ni and Pt molar fraction measured by Energy Dispersive Spectra (EDS) for [Cl-BzPy][Ni_xPt_{1-x}(mnt)₂] (x = 0.09-0.91).

| x | 0.09 | 0.21 | 0.34 | 0.42 | 0.54 | 0.64 | 0.73 | 0.84 | 0.91 |
|-----|-------|-------|-------|-------|-------|-------|-------|-------|-------|
| Ni% | 8.33 | 17.16 | 25.77 | 33.69 | 42.10 | 50.24 | 60.60 | 70.38 | 78.12 |
| Pt% | 91.67 | 82.84 | 74.23 | 66.31 | 57.90 | 49.76 | 39.40 | 29.62 | 21.88 |

Table S3 Ni and Pt molar fraction measured by Inductively coupled plasma-mass spectra (ICP-MS) for [Cl-BzPy][Ni_xPt_{1-x}(mnt)₂] (x = 0.09-0.91).

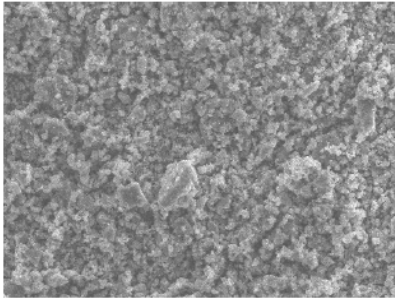
| Compound | Ni | Pt | Ni/Pt [#] | Ni/Pt [*] | Ni/Pt ^{**} |
|----------|-------|------|--------------------|--------------------|---------------------|
| x = 0.09 | 0.085 | 2.09 | 0.1359 | 0.1111 | 0.09695 |
| x = 0.21 | 0.48 | 5.35 | 0.2997 | 0.25 | 0.26526 |
| x = 0.34 | 1.22 | 8.77 | 0.4647 | 0.4286 | 0.50625 |
| x = 0.42 | 0.59 | 2.5 | 0.7884 | 0.6667 | 0.7347 |
| x = 0.54 | 2.11 | 6.22 | 1.1333 | 1 | 1.15285 |
| x = 0.64 | 1.03 | 2.11 | 1.6308 | 1.5 | 1.74033 |
| x = 0.73 | 2.1 | 2.45 | 2.8635 | 2.3333 | 2.64977 |
| x = 0.84 | 4.22 | 3.06 | 4.6071 | 4 | 5.43625 |
| x = 0.91 | 5.47 | 1.93 | 9.4683 | 9 | 10.73985 |

[#] ICP; ^{*}the molar ratio in the starting materials; ^{**}the molar ratio from occupation factors

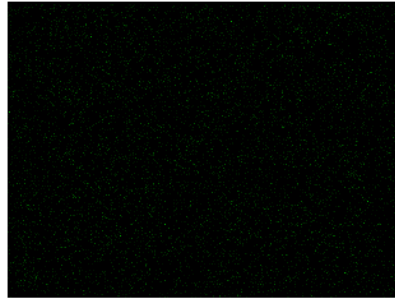
Table S4 Crystal structure of [Cl-BzPy][Ni_xPt_{1-x}(mnt)₂] (x = 0.09, 0.54 and 0.91) at 100 K

| Compound | x = 0.09 | x = 0.54 | x = 0.91 |
|-------------------------|---------------|-------------|---------------|
| Temp. (K) | | 100 | |
| Wavelength | | 0.71073 | |
| Formula weight | 667.67 | 601.00 | 556.34 |
| CCDC no. | 893368 | 893369 | 893370 |
| Crystal system | | Triclinic | |
| Space group | | P-1 | |
| a(Å) | 7.1590(2) | 7.1472(8) | 7.1912(2) |
| b(Å) | 12.2601(4) | 12.1875(11) | 12.0953(6) |
| c(Å) | 26.4337(11) | 26.268(2) | 26.0555(12) |
| α(°) | 87.472(3) | 87.956(7) | 88.532(4) |
| β(°) | 85.016(3) | 85.550(8) | 86.554(3) |
| γ(°) | 75.650(3) | 76.447(9) | 77.252(3) |
| V(Å ³),Z | 2238.59(13)/4 | 2217.3(4)/4 | 2206.26(16)/4 |
| ρ (g·cm ⁻¹) | 1.981 | 1.800 | 1.675 |
| F(000) | 1282 | 1184 | 1118 |

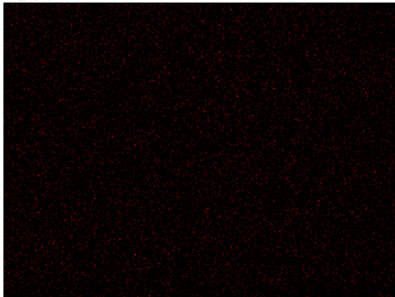
| | | | |
|--|---|----------------------------------|----------------------------------|
| Abs.coeff. (mm ⁻¹) | 6.286 | 3.681 | 1.904 |
| θ Range for data collection (°) | 2.99-26.00 | 2.99-26.00 | 2.99-26.00 |
| Index ranges | -9<h<8, -14<k<15, -27<l<32 | -8<h<8, -15<k<14, -32<l<32 | -8<h<8, -14<k<14, -32<l<24 |
| Rint | 0.1027 | 0.1055 | |
| Independent reflect. /restraints/parameters | 8775 / 0 / 555 | 8684 / 12 / 361 | 8643 / 0 / 560 |
| Refinement method | Full-matrix least-squares on F ² | | |
| Goodness of fit on F2 | 1.277 | 1.142 | 1.121 |
| R1, wR2a [I>2 σ (I)] | R1 = 0.1396 wR2 = 0.3277 | R1 = 0.2621 wR2 = 0.5928 | R1 = 0.2430 wR2 = 0.5535 |
| R1, wR2a [all data] | R1 = 0.1548 wR2 = 0.3329 | R1 = 0.2751 wR2 = 0.5969 | R1 = 0.2537 wR2 = 0.5572 |
| Residual (e·Å ⁻³) | 5.225/-11.153 | 10.100/-9.063 | 4.569/-5.279 |



电子图像 1

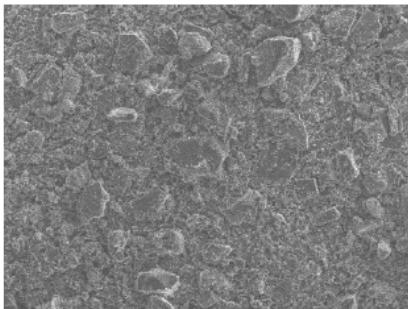


Ni Ka1

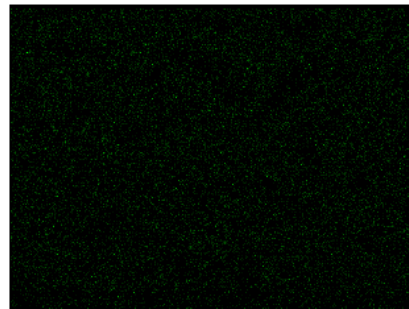


Pt La1

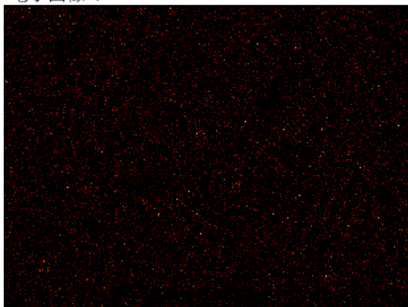
01 EDS elemental mapping of Ni, Pt in x = 0.09 sample



电子图像 1



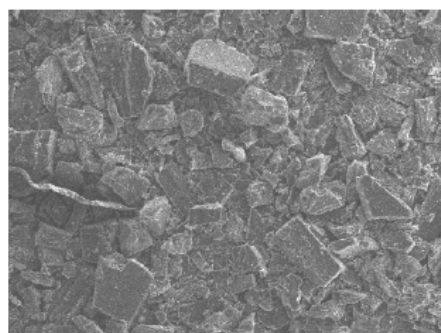
Ni Ka1



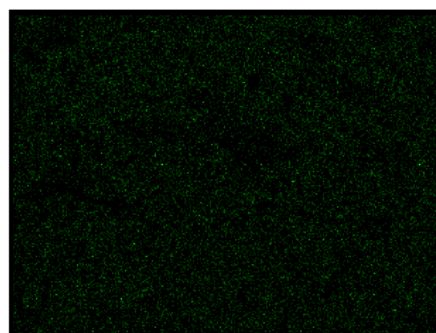
Pt La1

注释: 02 EDS elemental mapping of Ni, Pt in x = 0.54 sample





电子图像 1



Ni Ka1



Pt La1

注释: 03 EDS elemental mapping of Ni, Pt in x = 0.91 sample



Figure S2 EDS mappings of Ni and Pt in $[\text{Cl-BzPy}][\text{Ni}_x\text{Pt}_{1-x}(\text{mnt})_2]$ ($x = 0.09, 0.54$ and 0.91).

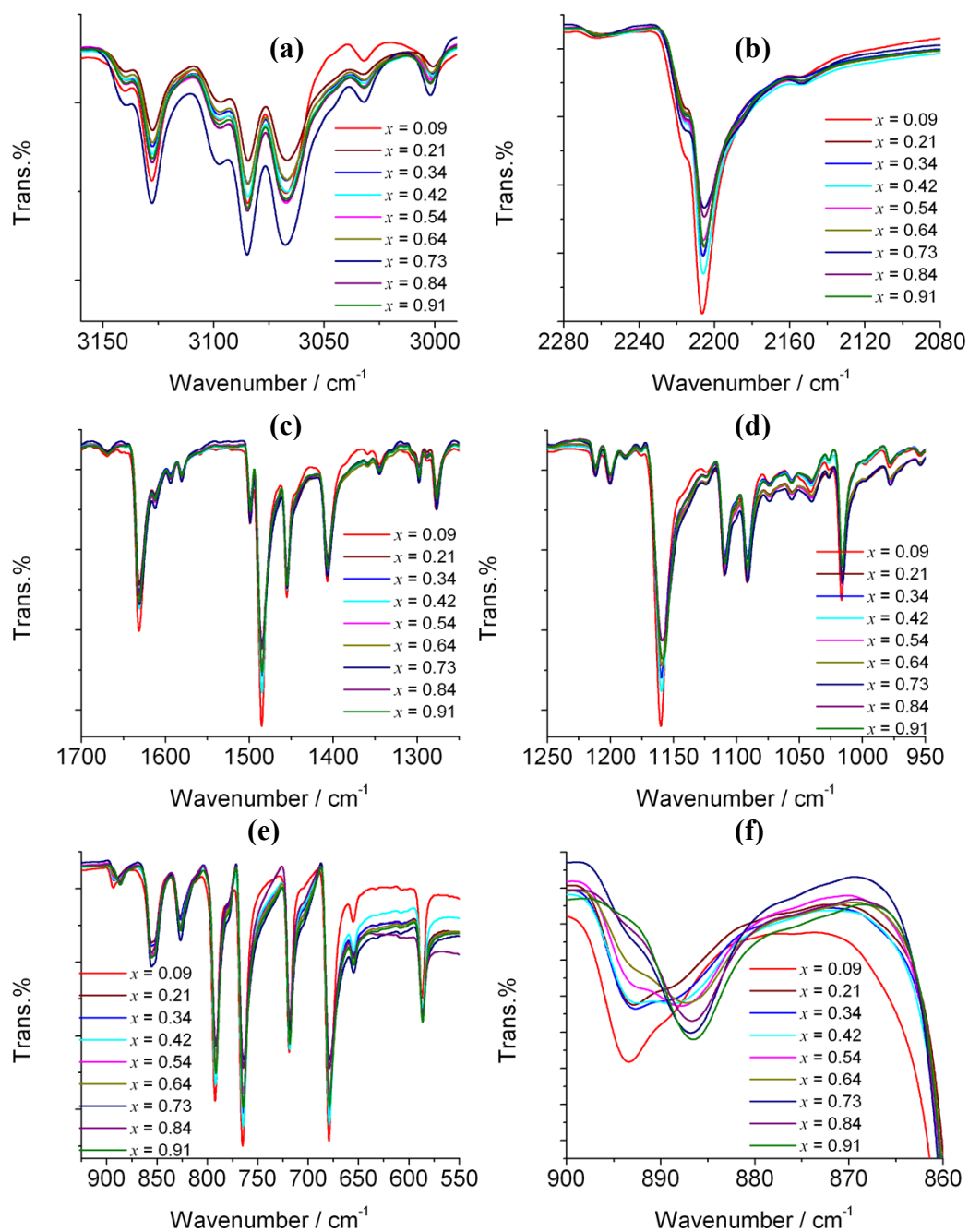


Figure S3 IR spectra for alloy compounds $[\text{Cl-BzPy}][\text{Ni}_x\text{Pt}_{1-x}(\text{mnt})_2]$ ($x = 0.09-0.91$) in the range 3190-550 cm^{-1} .

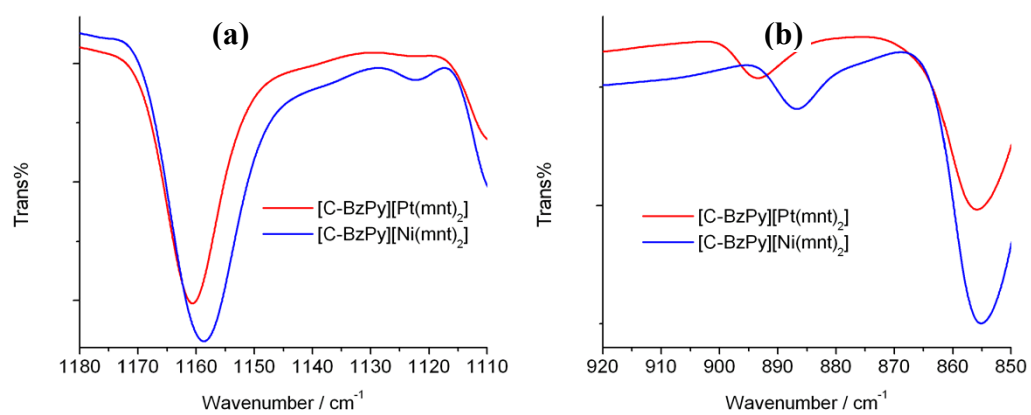
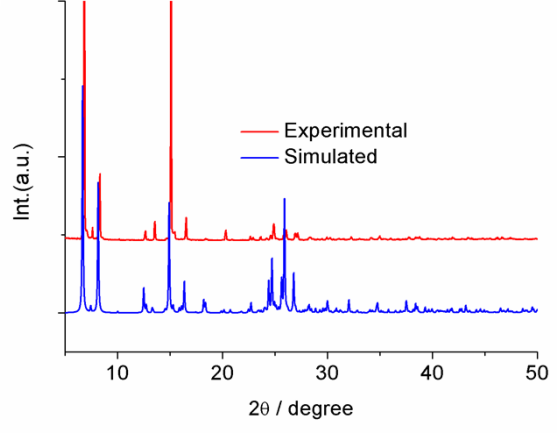
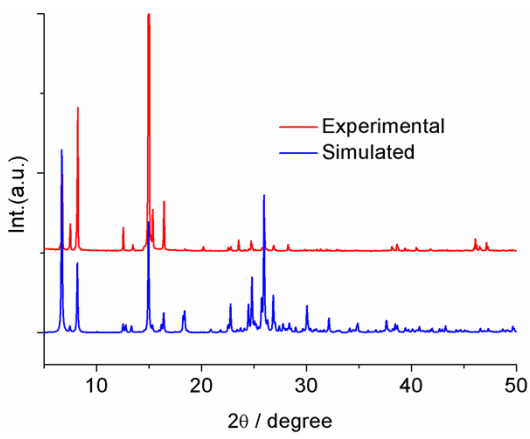
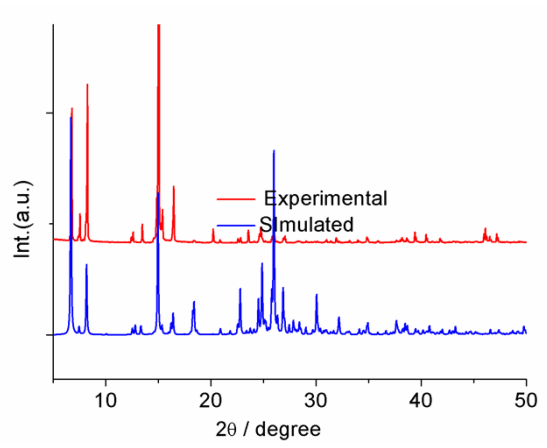
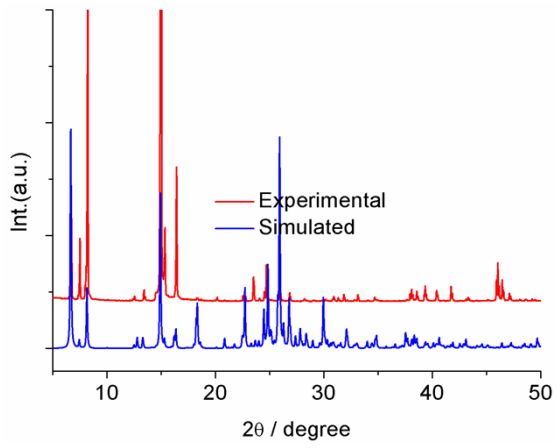
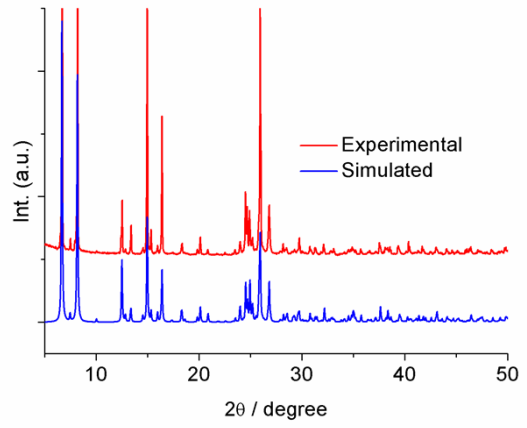
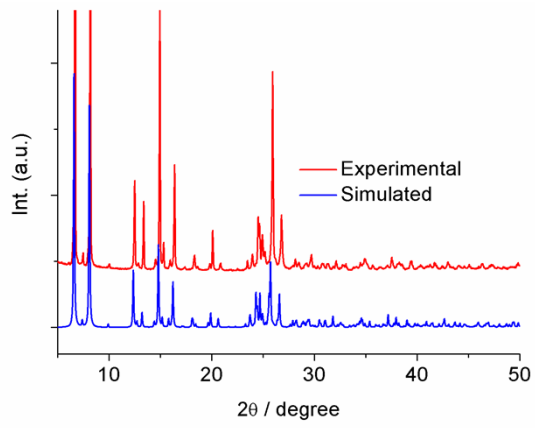


Figure S4 IR spectra of [Cl-BzPy][Ni(mnt)₂] and [Cl-BzPy][Pt(mnt)₂] (a) the band of $\nu_{C-S} + \nu_{C-C}$ and π_{C-CN} (b) the band of ν_{C-S} from mnt^{2-} ligand.



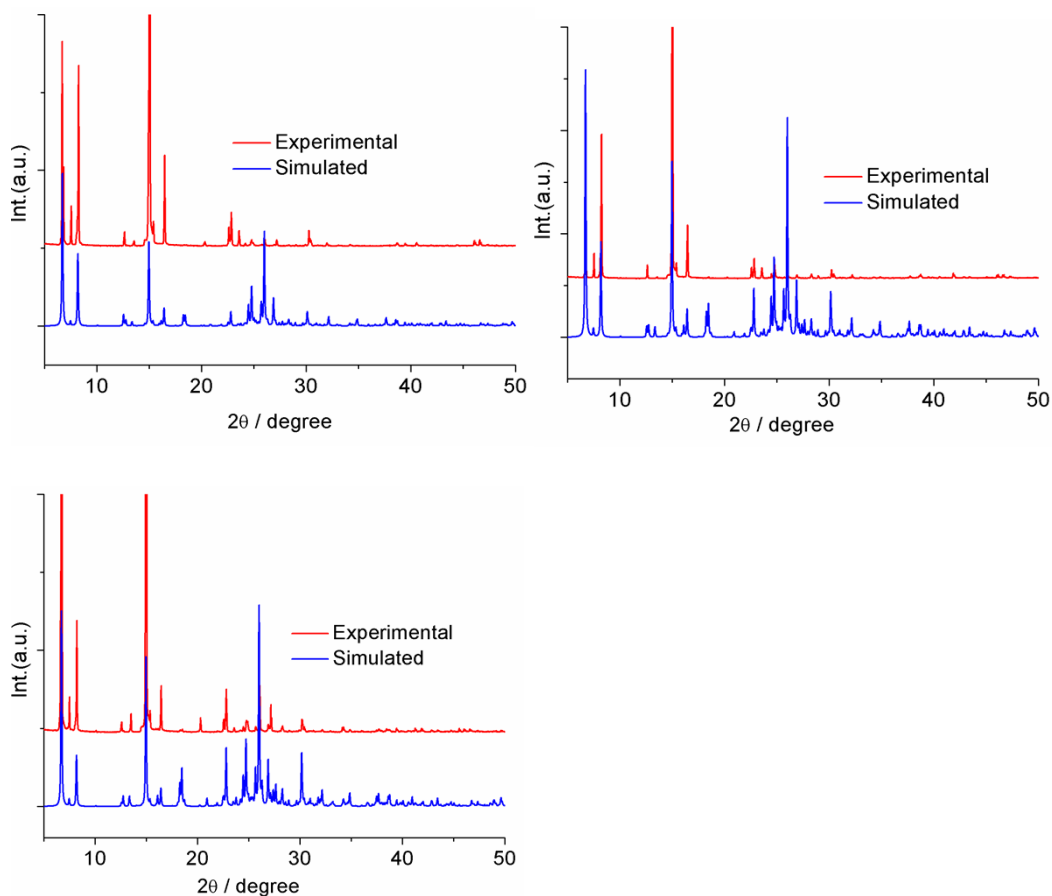


Figure S5 Simulated and Experimental Powder X-ray diffraction profiles for $x =$ (a) 0.09 (b) 0.21 (c) 0.34 (d) 0.42 (e) 0.54 (f) 0.64 (g) 0.73 (h) 0.84 (i) 0.91.

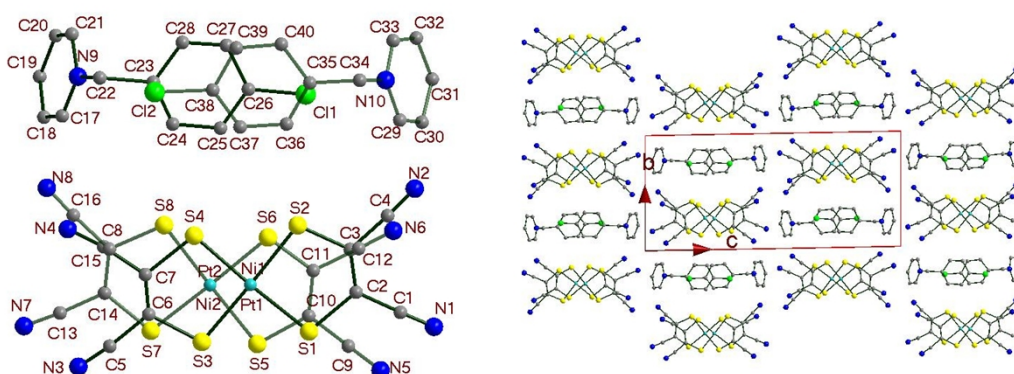


Figure S5 An asymmetric unit with non-H atoms labels and packing structure of $[\text{Cl-BzPy}][\text{Ni}_x\text{Pt}_{1-x}(\text{mnt})_2]$ ($x = 0.54$) viewed along a -axis at 100 K.